CrystEngComm

PAPER

Cite this: *CrystEngComm*, 2016, **18**, 7506

Peculiarities of styryl dyes of the benzoselenazole series crystal packings and their influence on solid phase [2 + 2] photocycloaddition reaction with single crystal retention†

Lyudmila G. Kuz'mina,*[a] Artem I. Vedernikov,[b] Judith A. K. Howard,[c] Stanislav I. Bezzubov,[a] Michael V. Alfimov[b] and Sergey P. Gromov*[b]

Received 23rd June 2016,
Accepted 21st August 2016

DOI: 10.1039/c6ce01426g

www.rsc.org/crystengcomm

New styryl dyes of the 2-benzoselenazole series which contain iodide, triiodide, and tosylate anions were synthesized. Crystals of these compounds were grown in different crystal forms – solvent free and hydroquinone, benzene or ethyl acetate solvated ones. X-ray structural studies of the crystals shows that those containing tosylate and triiodide anions form the centrosymmetrically related stacking motif, typical for styryl dye cations and favorable for [2 + 2] photocycloaddition (PCA) reactions. This reaction takes place in crystals with tosylate anions as a single crystal-to-single crystal process. On the contrary, in the triiodide dye crystals, the PCA reaction is lacking, probably due to a weak directional interaction of the selenium atoms with the anions. The iodide dye crystals demonstrate non-typical packing for styryl dyes and manifest as a two-dimensional close packing motif of the cations which is unfavorable for cycloaddition.

Introduction

A reversible photochemical reaction of [2 + 2] photocycloaddition (PCA) in ethylene compounds developed in 1960s to 1980s years of XX century[1–3] continues to create interest, not only as an accessible way to obtain cyclobutane derivatives,[4–32] but as a way of creating new optical materials.[33–36] Many investigations in this field have made it possible to establish a series of conditions and regularities to achieve PCA. In particular, this reaction proceeds in concentrated solutions and in the solid phase including single crystals under their irradiation with UV or visible light, and sometimes without single crystal decomposition. The last circumstance allows a fundamental study of topochemical processes in crystals using PCA transformations in crystals. This study is based on the previously established fact that the preorganization of ethylene moieties in the form of a parallel stacking dimer, with the distance (d) between ethylenic carbon atoms not exceeding 4.2 Å, is required to achieve PCA (Schmidt's criterion[1]) and that such a dimeric pair may exist in a crystal. A further study of the topochemical process involves an analysis of crystal packing and a significant target design is that the crystal packing supports isolated "pre-organized dimers" and hence the PCA reaction proceeds under irradiation of the initial crystals. X-ray structural analysis is the most efficient method to determine these metrics.

We chose brightly colored styryl dyes of general formula R–Het$^+$–HC=CH–ArX$^-$ (X$^-$ is a counterion) as objects of the study.

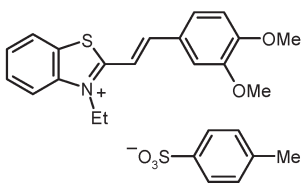

1

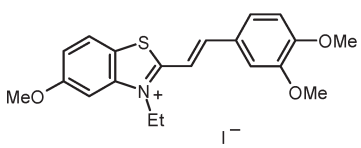

2

Scheme 1

[a] *N. S. Kurnakov Institute of General and Inorganic Chemistry, Russian Academy of Sciences, Leninsky prosp. 31, Moscow 119991, Russian Federation. E-mail: kuzmina@igic.ras.ru; Fax: +7 (495) 954 1279*
[b] *Photochemistry Center, Russian Academy of Sciences, Novatorov str. 7A-1, Moscow 119421, Russian Federation. E-mail: spgromov@mail.ru; Fax: +7 (495) 936 1255*
[c] *Department of Chemistry, Science Laboratories, University of Durham, South Road, Durham DH1 3LE, England, UK. E-mail: j.a.k.howard@durham.ac.uk*

† CCDC 1474550–1474556 and 1474558. For crystallographic data in CIF or other electronic format see DOI: 10.1039/c6ce01426g

Recently,[37,38] we published investigations of styryl dyes of the 2-benzothiazole series **1** and **2** (Scheme 1) in three crystal forms for each.

It has been found that in both dyes **1** and **2**, the PCA reaction proceeds as a single crystal-to-single crystal process in two of the crystal forms, whereas the third form turned out to be stable to irradiation with visible light. Ability of the styryl dyes to undergo solid phase PCA depends on crystal packing of the dye. In all cases, the cations in the crystals form centrosymmetrically related π-stacks, separated as dimeric pairs with the *syn*-head-to-tail mutual arrangement of the adjacent cations. With this arrangement, the ethylene bonds in a dimeric pair show separations of 3.53–3.81 Å. As a whole, this geometry is favorable for PCA. However, this reaction proceeds only in the pairs where heterocycle *N*-ethyl substituents are oriented away from the centre of the dimer. In the cases where these substituents are oriented towards the centre of the dimeric pair, the PCA reaction does not take place, apparently because of steric factors, since such an orientation of the substituents prevents ethylene groups from being sufficiently close to one another (Scheme 2).

We suggest that this structural peculiarity of the dimeric pair geometry influences the feasibility for the PCA reaction and therefore should be characteristic of not only the styryl dyes of the 2-benzothiazole series, but also of other styryl dyes involving *N*-substituents in the dye. In particular, styryl dyes of the 2-benzoselenazole series that are geometrically similar to dyes **1** and **2** and are of particular interest in this respect. On the other hand, a replacement of the sulfur atom in the dye by a selenium atom with higher polarizability and ability to enhance π–π interactions between the cations may lead to unexpected crystal packing which would prevent PCA. We were interested to study the ability of these compounds to form appropriate crystal packing motifs and to participate in PCA.

In this connection, we obtained three new dyes with the same cation and the following anions – iodide (dye **3**), triiodide (dye **4**), and tosylate (dye **5**) (Scheme 3). Their ability to undergo the PCA reaction in polycrystalline films and single crystals, with or without single crystal decomposition, was studied.

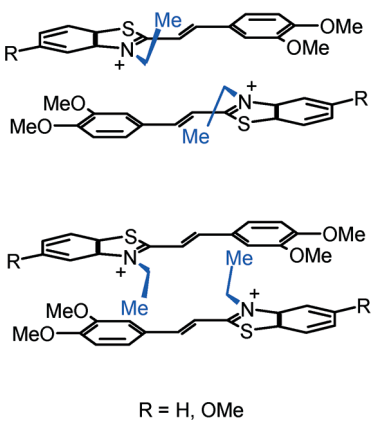

Scheme 2 Two possible orientations of *N*-ethyl substituents of the dye **1**, **2** cations with respect to centre of dimer.

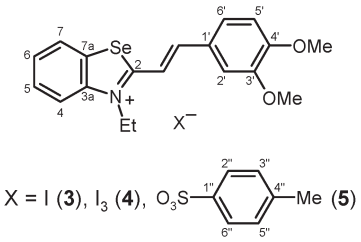

Scheme 3

Results and discussion

Synthesis of dye **3** was first attempted by a condensation of 3-ethyl-2-methylbenzoselenazolium iodide with 3,4-dimethoxybenzaldehyde in ethanol in the presence of pyridine. However, little separable mixture of the dye and compounds of undetermined composition (probably, the products of selenazole cycle opening) was obtained. Single crystals of dye **4** having triiodide anion were grown by slow crystallization of this mixture in MeCN–benzene solution. Apparently in the course of the synthesis, the iodide anions are partly oxidized with atmospheric oxygen with the formation of I_2. Dye **3** was successfully synthesized with 47% yield by a condensation of the reagents on heating in acetic anhydride. Dye **5** was obtained by melting **3** with ethyl 4-methylbenzenesulfonate (Scheme 4).

Irradiation with visible light of thin crystalline films of dyes **3** and **5** has shown that the PCA reaction proceeds only in the dye with the TsO^- anion. A centrosymmetric *rctt* isomer of the cyclobutane derivative **6** was produced and this was preceded by a *syn*-head-to-tail dimeric pair (Scheme 5).

The rate of the photoreaction in **5** turned out to be comparable with that in the related dye **1**;[37] under similar conditions (irradiation for 10 h) the extent of the conversion is 28% and 25%, respectively. We failed to convert dye **5** fully into the cyclobutane **6** and to characterize this product by physico-chemical methods. The reduction in the rate of photo-conversion of **5** under prolonged irradiation (^{1}H NMR control) as the product **6** was formed, was accompanied by the appearance of other compounds, which are probably products of isomerization and/or decomposition of **6**.

Crystals of dyes **3**–**5** have been grown from different solvent mixtures. We managed to obtain three crystal forms for

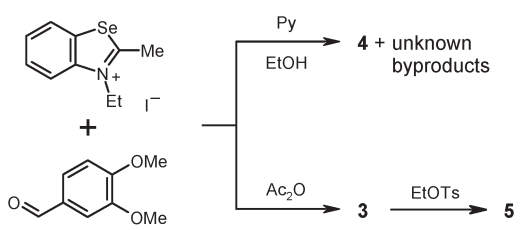

Scheme 4

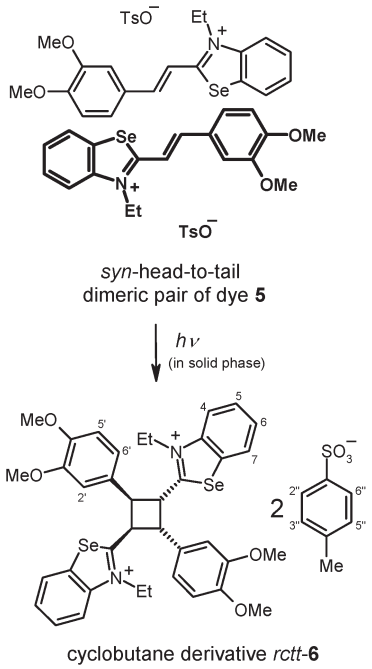

Scheme 5

3 (benzene solvate – **3a**, hydroquinone solvate – **3b**, and ethyl acetate–water solvate **3c**), one for **4**, and two for **5** (solvate free form **5** and water–hydroquinone solvate **5a**).

Structures of all crystals were determined by X-ray diffraction analysis. Fig. 1 shows asymmetric units for all the crystals.

The unit cell of **3a** contains two independent dye cations, two iodide anions, and solvate benzene molecule. The unit cell of **3b** involves two independent cations, two iodide anions, and one solvate hydroquinone molecule. The hydroquinone molecule is disordered over two positions with the 0.88 : 0.12 occupancies ratio. The independent part of **3c** involves one cation, one iodide anion, and two different solvate molecules, ethyl acetate and water, co-located near a symmetry centre with ratio of occupancies 0.5 : 0.3 respectively. The crystallographically independent part of unit cell of **4** consists of two cations and two triiodide anions. The unit cell of **5** involves one independent cation and one independent tosylate anion having rotational disorder of the SO_3 group over three positions with occupancies ratio 0.52 : 0.40 : 0.08. The unit cell of **5a** involves one independent cation, one anion, and solvate water and hydroquinone molecules.

The Se–C bond lengths are close in the all molecules and vary within 1.864–1.885 Å. In all the structures the Het–HC═CH–Ar fragment is near planar, the dihedral angle Het/Ar is equal to 4.1°/7.3°, 4.4°/9.6°, 4.2°, 5.1°/6.7°, 8.6°, 3.5°, respectively. In the ethylene fragment C1–C2═C3–C4, the length of the C2═C3 double bond [1.359(5)/1.345(6), 1.345(8)/1.348(9), 1.352(3), 1.344(4)/1.353(5), 1.348(4), 1.345(4) Å in **3a**, **3b**, **3c**, **4**, **5**, **5a**, respectively] is essentially localized, which is important for the PCA reaction to proceed.

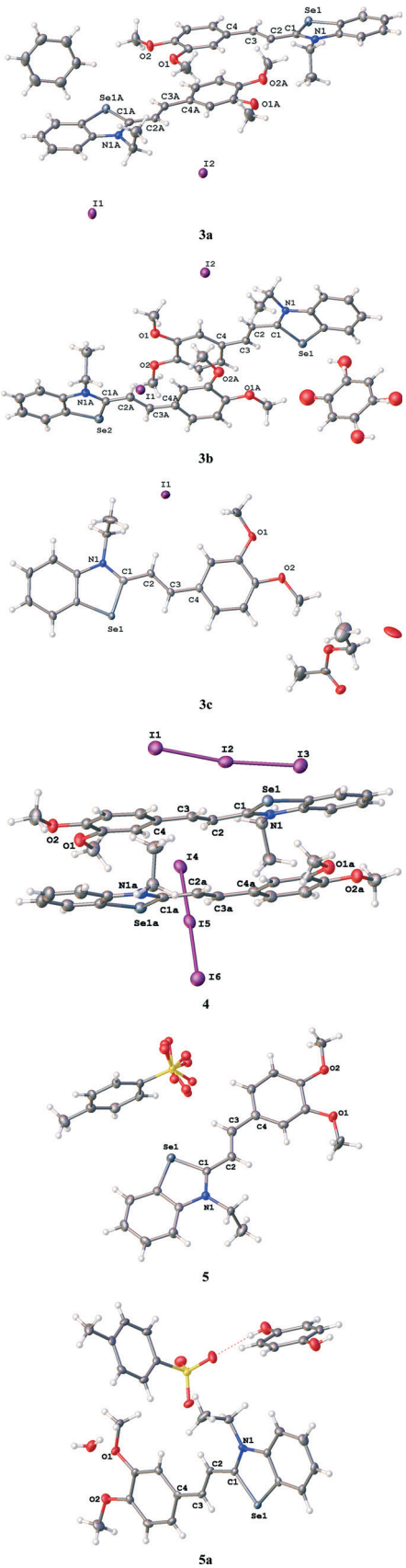

Fig. 1 The asymmetric units of crystals **3a**, **3b**, **3c**, **4**, **5**, and **5a**. Here and in the next figures all non-hydrogen atoms are drawn in thermal ellipsoids at the 50% probability level.

An irradiation of all investigated crystals with visible light for 12 h causes the PCA reaction in **5** and **5a**. This reaction proceeds with single crystal retaining and results in crystals **6** and **6a**, respectively. Crystals of **3c** decompose and the possible reasons for this may be the loss of solvate molecules or/and accomplishing PCA, but with destruction of the lattice. In the course of irradiation, the crystals of **3c** are first subjected to cracking and the resultant small crystals become amorphous. These observations suggest that both of these processes – solvent loss and PCA – have taken place. Crystals **3a**, **3b**, and **4** do not change during prolonged irradiation.

X-ray structures of **6** and **6a** are shown in Fig. 2.

In crystals of **5**, that do not contain any solvate molecules, the PCA reaction is accomplished fully. In crystals of **5a**, the reaction leads to a mixture of the initial dye and the cyclobutane *rctt*-**6**, with the molar ratio 6 : 1 (the degree of conversion is 25%). Further irradiation for more than a month does not result in any increase in the amount of **6** achieved.

Crystal packing of **5** shows stacks of cations separated by tosylate anions (Fig. 3). The packing stacking motif is controlled by π–π interactions between the centrosymmetrically related pairs of cationic structural units.[39,40] As a result, the mutual arrangement of the cations in a stack is *syn*-head-to-tail (Fig. 4).

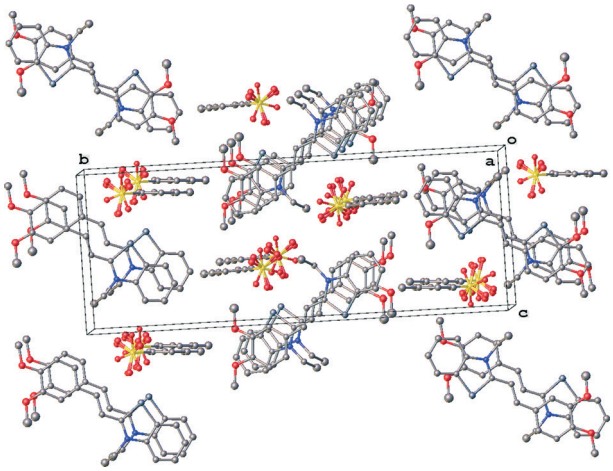

Fig. 3 Fragment of crystal packing of **5**; hydrogen atoms are omitted for clarity.

Within a stack, the distances between the ethylene carbon atoms (*d*) in successive pairs of cations alternate – 4.08 and 3.49 Å. Both distances satisfy the Schmidt's criterion.[1] However, only in pairs with shorter *d* the *N*-ethyl substituents are oriented out of the centres of the pairs, whereas in pairs with longer *d* they are oriented towards the pair centres. This means that PCA can be accomplished only in the pairs with shorter *d*, that is, only in crystallographically equivalent pairs of cations. For this reason, PCA in **5** can proceed without single crystal degradation.

The similar packing motif was observed for crystal **5a** (Fig. 5). In this packing isolated stacks of cations are surrounded by tosylate anions, hydroquinone, and water solvate molecules. The stack in **5a** also has *syn*-head-to-tail centrosymmetrically related arrangement with alternating distances in successive pairs of cations (Fig. 6).

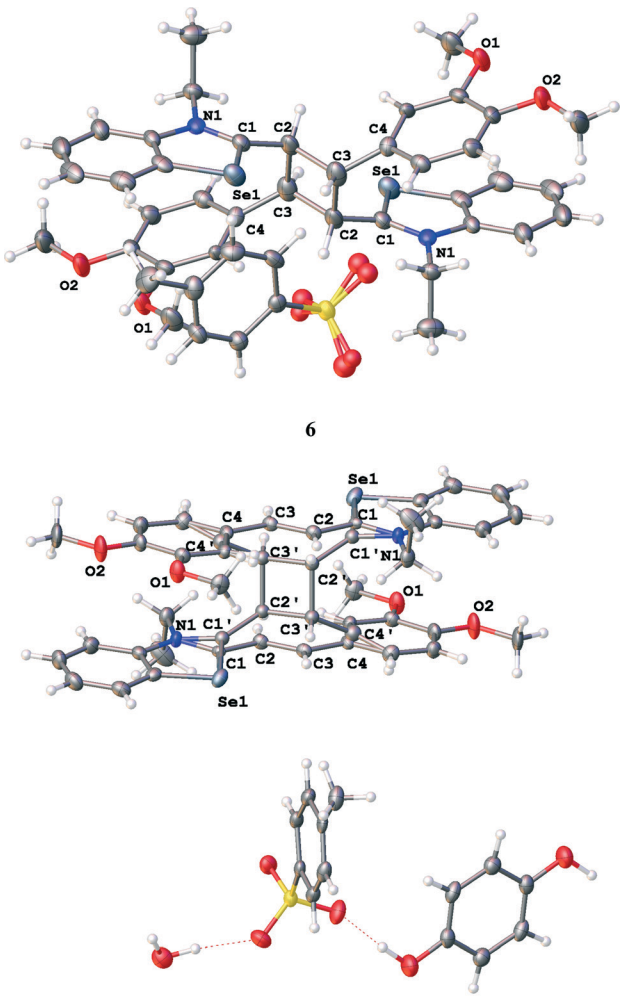

Fig. 2 The asymmetric units of crystals **6** and **6a**.

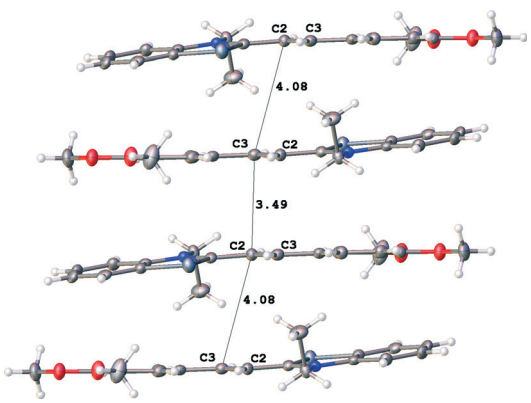

Fig. 4 Structure of a stack in **5**; here and in the next figures distances are given in Å.

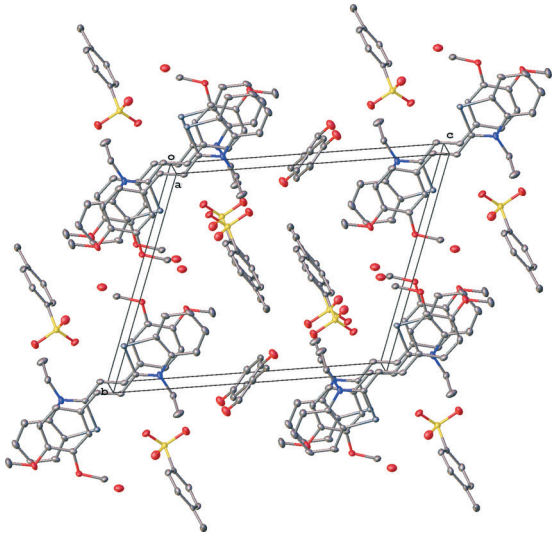

Fig. 5 Crystal packing of **5a**.

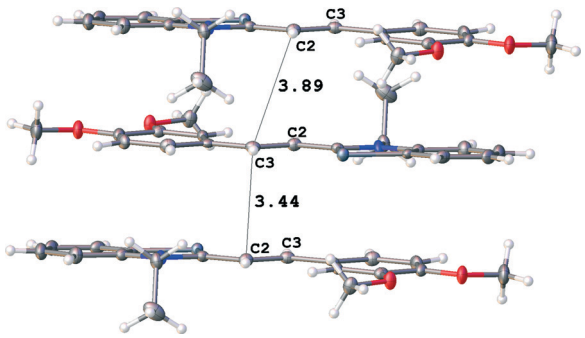

Fig. 6 The structure of a stack in **5a**.

Both distances (3.89 and 3.44 Å) also satisfy the Schmidt's criterion and the shorter of them is observed in the pair, where the *N*-ethyl substituents are oriented out of the centre of the pair.

A difference between the two crystal packings consists in the occurrence of solvate molecules in **5a** and their lacking in **5**. The solvate molecules in **5a** participate in the formation of a system of hydrogen bonds (Fig. 7).

These interactions fix a definite orientation of the SO_3 group of anion unlike the situation in crystal structure **5** where this group reveals a rotational disorder. The hydrogen bond occurrence makes the structure **5a** more rigid compared to **5**. Apparently, for this reason the PCA reaction in **5a** goes more slowly and not fully. In crystals **5** the disorder of SO_3 group of the anion is indicative of its free rotation about the C–S bond. This rotation may be accomplished synchronously with the atomic displacements in the course of PCA thus to accelerate this transformation. By contrast, the positions of the SO_3 group in **5a** are fixed by hydrogen bonds and this somewhat hinders the PCA transformation.

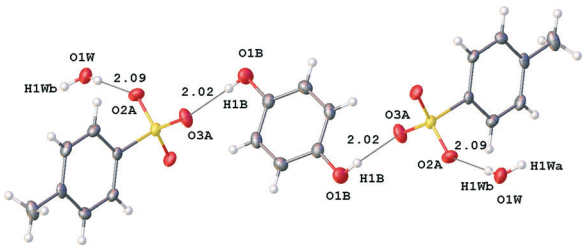

Fig. 7 System of hydrogen bonds in crystal packing of **5a**.

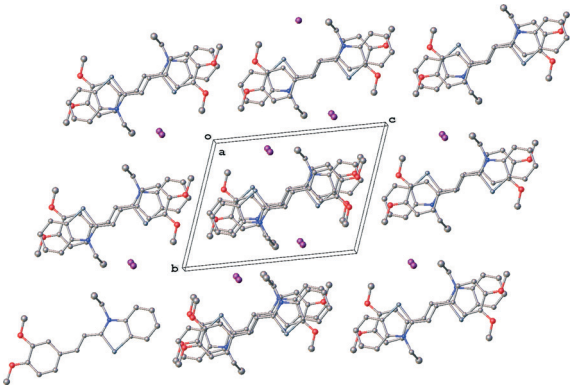

Fig. 8 Crystal packing of **3c**; hydrogen atoms and solvate molecules are omitted for clarity.

The crystal packing of **3c** is also formed of stacks of cations separated by solvate molecules and iodide anions (Fig. 8). It should be noted that the solvate molecules of ethyl acetate are situated in large cavities within the crystal packing and therefore they have only a few contacts with adjacent structural units. For this reason, easy elimination of solvate molecules may take place on crystal storage and especially during their irradiation that is accompanied by crystal warming. Indeed, an incandescent 60 W lamp was used for crystal irradiation at distance of ~15 cm.

The stacks in **3c** also have *syn*-head-to-tail arrangement with alternating distances *d* (Fig. 9).

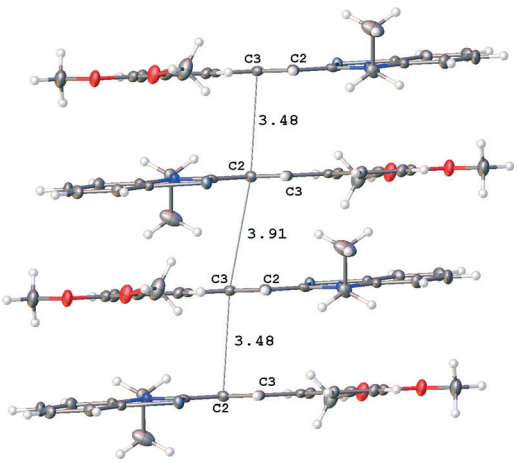

Fig. 9 Stack of cations in **3c**.

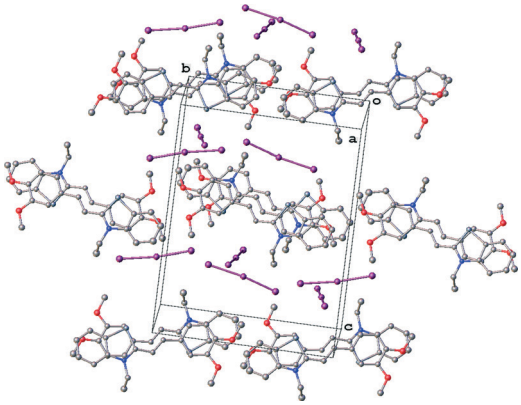

Fig. 10 Crystal packing of **4**; hydrogen atoms are omitted for clarity.

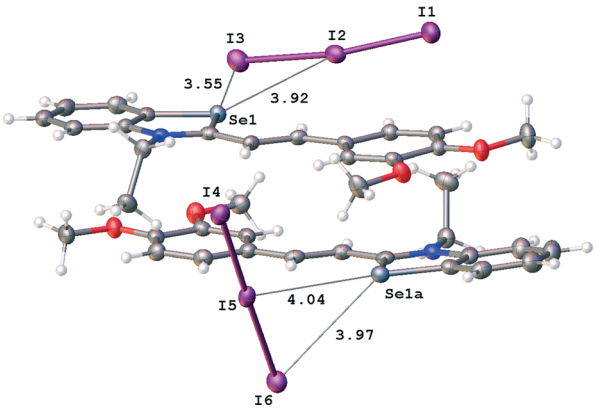

Fig. 12 Short contacts between selenium and iodine atoms in **4**.

This crystal packing is also favorable for PCA and this reaction proceeds in the crystals together with their decomposition, due to solvate elimination.

Crystal packing of **4** is also built of analogous isolated stacks of cations separated by I_3^- anions (Fig. 10).

The stacks in **4** have a more complicated structure since it involves two crystallographically independent cations (Fig. 11) arranged in a sequence –B–B–A–A–B–B– (A and B – crystallographically independent cations).

The most favorable geometry of a cation pair for PCA to proceed is observed for a centrosymmetric pair of cations formed by crystallographically independent cations with dashed atom numbering (*e.g.* B–B). Nevertheless, PCA was not observed in this crystal even after prolonged irradiation for more than a month. The real reason for high stability of the crystal to irradiation may be connected with two factors. One of them is that only in one of three independent pairs of cations in a stack is this reaction possible. Another one is the weak interactions between the I_3^- anions and the selenium atoms (Fig. 12). The distances between iodine and selenium atoms are rather short. The Cambridge Crystallographic Database contains 111 entries for structures with Se···I contacts; the maximum of this contact distribution in the range 3.5–4.5 Å accounts for 4.1 Å.

In both structures **3a** and **3b** identical complicated packing motifs were found. This packing motif for **3a** is shown in Fig. 13.

The crystal packing differs from those earlier observed for all crystals of styryl dyes. Earlier we showed that six canonical packing motifs exist for planar conjugated molecules and molecular cations (Fig. 14), four of which (1–4) are favorable for PCA.[21,38,41–43]

In the packing motifs 1–4 (Fig. 14) isolated stacks or stacking dimeric pairs of cations occur, which themselves do not form any π-stacking interactions with the adjacent stacks or dimeric pairs.

In crystal packing of **3a** and **3b** cations form layers that alternate with layers of anions and solvate molecules. The structures of the layers in **3a** and **3b** are shown in Fig. 15 and 16, respectively.

In both cases the pre-organized dimeric pairs may be selected, with very short distances between the ethylene bonds

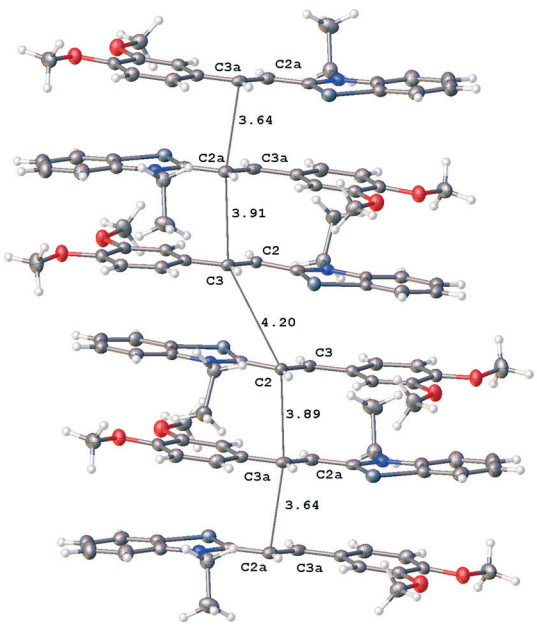

Fig. 11 Stack of cations in **4**.

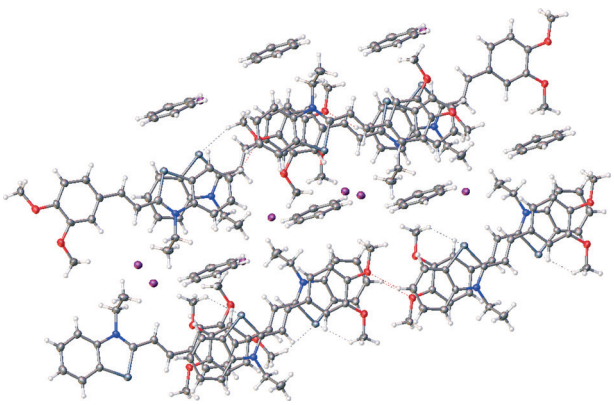

Fig. 13 Fragment of crystal packing of **3a**.

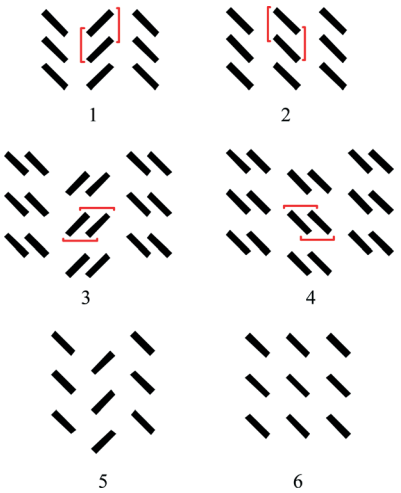

Fig. 14 Canonical types of crystal packings of flat conjugated molecules; the lines represent projections of the molecules; the red brackets indicate the dimeric pairs.

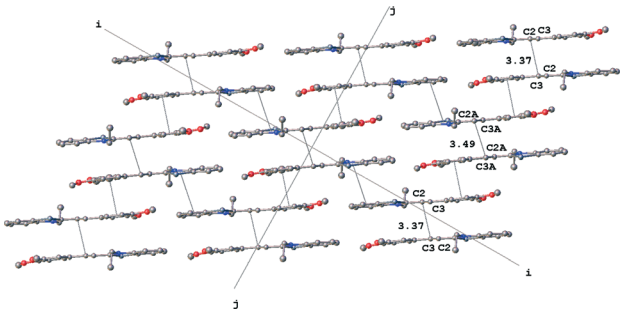

Fig. 15 Structure of cation layer in **3a**.

of the cations (3.36–3.50 Å) and be composed of crystallographically independent units. These short distances indicate a strong π–π interaction in the dimeric pairs. However, these dimeric pairs may be simultaneously related to two different stacks running along two crossed directions – *ii* and *jj* (see Fig. 15). Interplanar distances between heterocyclic systems of adjacent dimeric pairs 3.83 Å and between aryl rings 3.44 Å correspond to π–π interactions. This means that any "pre-organized dimer" participates in a stacking interaction not only in one stack running along the *ii* direction, but also in another crossed stack running along the *jj* direction (see Fig. 15).

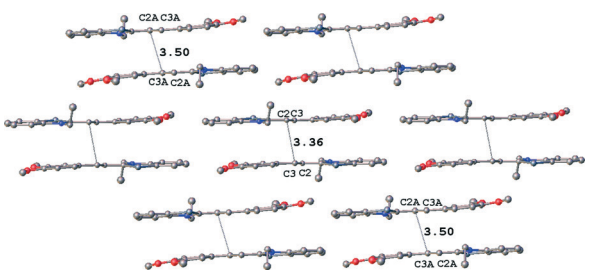

Fig. 16 Structure of cation layer in **3b**.

Thus, an inclusion of the Se atom in a heterocycle instead of the S atom may result in forming a crystal packing motif non-typical for planar conjugated molecules that had not been observed earlier for styryl dyes and styryl heterocycles.

Conclusions

Crystal packings of styryl dyes **3c**, **4**, **5**, and **5a** containing I^-, I_3^-, and tosylate anions are favorable for [2 + 2] photocycloaddition (PCA). In **5** and **5a** this reaction is accomplished as a single crystal-to-single crystal process. In **5** this process is facilitated by synchronous process of atomic displacements in cations in the course of PCA and rotation of SO_3 fragments in anions. An occurrence of weak secondary bonds between Se and I atoms in **4** prevents PCA from accomplishing. On irradiation, the crystals **3c** decompose because of both an elimination of solvent molecules (ethyl acetate and water) and PCA accomplishment.

Crystals **3a** and **3b** demonstrate a non-typical crystal packing motif for a planar conjugated molecular system unfavorable for PCA due to a tendency of selenium compounds to form two-dimensional systems of π–π stacking interactions.

Experimental section

General

The melting points (uncorrected) were measured in capillaries on a Mel-Temp II apparatus. ^{1}H and ^{13}C NMR spectra were recorded on a Bruker DRX500 instrument (500.13 and 125.76 MHz, respectively) in DMSO-d_6 at 25 °C using the solvent as an internal standard (δ_H 2.50 ppm and δ_C 39.43 ppm). 2D NOESY and heteronuclear correlation (HSQC and HMBC) spectra were used to assign the proton and carbon signals (atom numbering is shown in Schemes 3 and 5). The absorption spectra of solutions of dyes **3** and **5** ($C = 2 \times 10^{-5}$ M) in acetonitrile were measured on a Cary 4000 spectrophotometer (Agilent) in a range of 200–600 nm (at an interval of 1 nm) in 1 cm quartz cells. The elemental analysis was performed in the Laboratory of Microanalysis of A. N. Nesmeyanov Institute of Elementoorganic Compounds of the Russian Academy of Sciences (Moscow, Russian Federation). The samples for elemental analysis were dried at 80 °C *in vacuo*.

Preparations

3,4-Dimethoxybenzaldehyde and ethyl 4-methylbenzenesulfonate were purchased from "Sigma-Aldrich". 3-Ethyl-2-methyl-1,3-benzoselenazol-3-ium iodide was prepared according to a published procedure.[44]

2-[(*E*)-2-(3,4-Dimethoxyphenyl)vinyl]-3-ethyl-1,3-benzoselenazol-3-ium iodide (3). A mixture of 3-ethyl-2-methyl-1,3-benzoselenazol-3-ium iodide (227 mg, 0.65 mmol), 3,4-dimethoxybenzaldehyde (161 mg, 0.97 mmol), and acetic anhydride (3 mL) was heated at 140 °C (oil bath) in darkness for 14 h. The solvent was evaporated *in vacuo* and the black residue was dissolved in MeOH (5 mL) at heating. After

cooling to −10 °C, a precipitate thus formed was filtered off, washed with cold MeOH (4 × 1.5 mL) and dried in air in darkness to give dye **3** (152 mg, yield 47%) as a red-brown powder, mp 221–223 °C (dec.). Calcd. for $C_{19}H_{20}INO_2Se$: C, 45.62; H, 4.03; N, 2.80. Found: C, 45.46; H, 4.09; N, 2.76%. ^{1}H NMR: δ = 1.46 (t, J = 7.2 Hz, 3 H, *Me*CH_2), 3.89 (s, 3 H, 4′-MeO), 3.90 (s, 3 H, 3′-MeO), 4.95 (q, J = 7.2 Hz, 2 H, CH_2N), 7.16 (d, J = 8.5 Hz, 1 H, 5′-H), 7.68 (br s, 1 H, 2′-H), 7.69–7.73 (m, 2 H, 6-H, 6′-H), 7.81 (m, 1 H, 5-H), 7.86 (d, J = 15.5 Hz, 1 H, HC═C*H*Het), 8.24 (d, J = 8.5 Hz, 1 H, 4-H), 8.27 (d, J = 15.5 Hz, 1 H, *H*C═CHHet), 8.44 (dd, J = 8.1 Hz, J = 0.8 Hz, 1 H, 7-H) ppm. ^{13}C NMR: δ = 14.04 (*Me*CH_2), 45.22 (CH_2N), 55.82 (4′-MeO), 56.00 (3′-MeO), 111.70 (5′-C), 111.92 (2′-C), 113.39 (HC═*C*HHet), 117.91 (4-C), 125.79 (6′-C), 127.19 (1′-C), 127.33 (7-C), 127.78 (6-C), 128.86 (5-C), 129.75 (7a-C), 142.09 (3a-C), 149.03 (3′-C), 151.54 (H*C*═CHHet), 152.97 (4′-C), 180.71 (2-C) ppm. UV–vis (MeCN): λ_{max} = 437 nm (ε = 33 800 M^{-1} cm^{-1}).

2-[(*E*)-2-(3,4-Dimethoxyphenyl)vinyl]-3-ethyl-1,3-benzoselenazol-3-ium 4-methylbenzenesulfonate (5). A mixture of compound **3** (50.7 mg, 0.101 mmol) and ethyl 4-methylbenzenesulfonate (101.4 mg, 0.507 mmol) was heated at 120 °C (oil bath) in darkness for 5 h. After cooling to room temperature, the reaction mixture was washed with benzene (6 × 2 mL) and the insoluble substance was dried in air in darkness to give dye **5** (41.2 mg, yield 75%) as an orange-brown powder, mp 231–234 °C. Calcd. for $C_{26}H_{27}NO_5SSe$: C, 57.35; H, 5.00; N, 2.57. Found: C, 57.17; H, 5.03; N, 2.59%. ^{1}H NMR: δ = 1.46 (t, J = 7.2 Hz, 3 H, *Me*CH_2), 2.28 (s, 3 H, *Me*Ar), 3.89 (s, 3 H, 4′-MeO), 3.90 (s, 3 H, 3′-MeO), 4.95 (q, J = 7.2 Hz, 2 H, CH_2N), 7.11 (d, J = 8.0 Hz, 2 H, 3″-H, 5″-H), 7.16 (d, J = 8.2 Hz, 1 H, 5′-H), 7.47 (d, J = 8.0 Hz, 2 H, 2″-H, 6″-H), 7.68 (br s, 1 H, 2′-H), 7.69–7.73 (m, 2 H, 6-H, 6′-H), 7.81 (m, 1 H, 5-H), 7.86 (d, J = 15.4 Hz, 1 H, HC═C*H*Het), 8.24 (d, J = 8.6 Hz, 1 H, 4-H), 8.27 (d, J = 15.4 Hz, 1 H, *H*C═CHHet), 8.44 (d, J = 8.1 Hz, 1 H, 7-H) ppm. ^{13}C NMR: δ = 14.00 (*Me*CH_2), 20.67 (*Me*Ar), 45.17 (CH_2N), 55.79 (4′-MeO), 55.91 (3′-MeO), 111.71 (5′-C), 111.88 (2′-C), 113.42 (HC═*C*HHet), 117.93 (4-C), 125.41 (2″-C, 6″-C), 125.80 (6′-C), 127.22 (7-C, 1′-C), 127.81 (6-C), 127.93 (3″-C, 5″-C), 128.86 (5-C), 129.80 (7a-C), 137.45 (4″-C), 142.08 (3a-C), 145.74 (1″-C), 149.08 (3′-C), 151.58 (H*C*═CHHet), 153.00 (4′-C), 180.86 (2-C) ppm. UV–vis (MeCN): λ_{max} = 437 nm (ε = 35 300 M^{-1} cm^{-1}).

2,2′-[2-*c*,4-*t*-Bis(3,4-dimethoxyphenyl)cyclobutane-1-*r*,3-*t*-diyl]bis(3-ethyl-1,3-benzoselenazol-3-ium) bis(4-methylbenzenesulfonate) (*rctt*-6). An emulsion of dye **5** (18.2 mg, 33.5 μmol) in MeCN (0.5 mL) was evaporated in a glass Petri dish to form a thin polycrystalline film of the dye (spot diameter ~7 cm). The obtained sample was irradiated with light from an incandescent lamp (60 W) from a distance of ~15 cm for 100 h. During the experiment, samples were mechanically taken several times to study the film composition by the ^{1}H NMR method (the spectra were recorded immediately after the samples were dissolved in DMSO-d_6; this is necessary because of the fairly fast isomerization of the *rctt* isomers of cyclobutane obtained from the styryl dyes of similar structure[45]).

An analysis of the ratio of integral intensities of the same type signals from dye **5** and cyclobutane *rctt*-**6** showed that the degree of phototransformation within 10 h was 28%, that within 40 h was 51%, and that within 100 h was 63%. The last sample contained also an impurity of unknown byproducts (~20 mol%), which probably are products of solid-phase isomerization of *rctt*-**6** and/or its destruction.

Table 1 X-ray structure determination summary for **3a**, **3b**, **3c**, and **4**

Compound	**3a**	**3b**	**3c**	**4**
Solvate	0.5C_6H_6	0.5$C_6H_6O_2$	0.5EtOAc + 0.3H_2O	
Empirical formula	$C_{22}H_{23}INO_2Se$	$C_{22}H_{23}INO_3Se$	$C_{21}H_{24.3}INO_{3.3}Se$	$C_{19}H_{20}I_3NO_2Se$
M	539.27	555.27	549.09	754.05
Crystal system	Triclinic	Triclinic	Triclinic	Monoclinic
Space group	$P\bar{1}$	$P\bar{1}$	$P\bar{1}$	$P2_1/c$
a/Å	11.6009(7)	11.8766(3)	7.3704(4)	15.2110(3)
b/Å	13.0363(8)	12.7576(4)	10.8423(5)	14.7644(3)
c/Å	15.2941(9)	15.3353(4)	14.5069(7)	21.064(4)
α/°	106.333(2)	105.4770(10)	107.977(2)	90
β/°	96.656(2)	97.1060(10)	100.703(2)	108.775(1)
γ/°	106.040(2)	105.1850(10)	93.136(2)	90
V/Å^3	2085.7(2)	2113.78(10)	1075.69(9)	4478.89(16)
Z	4	4	2	8
μ/mm^{-1}	3.297	3.259	3.202	5.825
Crystal size/mm^3	0.33 × 0.07 × 0.06	0.38 × 0.32 × 0.30	0.08 × 0.07 × 0.06	0.56 × 0.14 × 0.05
Colour	Red	Red	Red	Violet
T/K	120	120	120	120
Data collected	31 365	25 381	15 978	51 154
Unique data (R_{int})	10 980 (0.098)	11 152 (0.0160)	4342 (0.0286)	13 042 (0.0481)
2θ range/°	2.43–29.00	2.82–29.00	2.83–26.50	2.82–30.00
No. of variables	493	511	279	474
R_1 [$I > 2\sigma(I)$]	0.0619	0.0258	0.0234	0.0283
wR_2 (all data)	0.1586	0.0331	0.0461	0.0543
GOF	1.038	1.020	1.032	0.893
$\Delta\rho_{max,min}$/e Å^{-3}	2.10/−0.95	1.30/−1.00	0.61/−0.56	1.53/−1.17

Table 2 X-ray structure determination summary for **5**, **5a**, **6**, and **6a**

Compound	**5**	**5a**	**6**	**6a**
Solvate		$0.5C_6H_6O_2 + H_2O$		$0.5C_6H_6O_2 + H_2O$
Empirical formula	$C_{26}H_{27}NO_5SSe$	$C_{29}H_{32}NO_7SSe$	$C_{52}H_{54}N_2O_{10}S_2Se_2$	$C_{29}H_{32}NO_7SSe$
M	544.51	617.58	1089.02	617.58
Crystal system	Monoclinic	Triclinic	Monoclinic	Triclinic
Space group	$P2_1/n$	$P\bar{1}$	$P2_1/n$	$P\bar{1}$
a/Å	7.2116(4)	7.2613(3)	7.5964(7)	7.2675(2)
b/Å	29.2202(16)	12.9355(7)	29.113(3)	12.9365(6)
c/Å	11.1130(6)	15.3053(9)	10.9942(9)	15.3429(6)
α/°	90	109.055(5)	90	108.909(4)
β/°	93.721(5)	92.175(4)	96.454(4)	92.576(3)
γ/°	90	96.618(4)	90	96.008(3)
V/Å^3	2437.3(2)	1345.40(13)	2416.0(4)	1352.36(9)
Z	4	2	2	2
μ/mm^{-1}	1.664	1.523	1.679	1.515
Crystal size/mm^3	0.46 × 0.12 × 0.08	0.44 × 0.42 × 0.14	0.46 × 0.12 × 0.08	0.44 × 0.42 × 0.14
Color	Orange	Orange	Orange	Orange
T/K	120	120	120	120
Data collected	16 092	11 336	19 914	24 708
Unique data (R_{int})	5302 (0.0661)	5555 (0.0456)	6401 (0.1449)	6214 (0.0782)
2θ range/°	2.78–27.00	2.53–27.00	2.80–29.00	2.76–27.00
No. of variables	316	364	305	382
R_1 [$I > 2\sigma(I)$]	0.0520	0.0396	0.0557	0.0535
wR_2 (all data)	0.1078	0.0921	0.0813	0.1140
GOF	0.962	1.045	0.724	1.097
$\Delta\rho_{max,min}$/e Å^{-3}	0.54/−0.55	1.28/−0.43	0.55/−0.48	1.44/−1.70

^{1}H NMR for *rctt*-**6**: δ = 1.36 (t, J = 7.1 Hz, 6 H, 2 *Me*CH$_2$), 2.28 (s, 6 H, 2 *Me*Ar), 3.66 (s, 6 H, 2 MeO), 3.70 (s, 6 H, 2 MeO), 4.50–4.59 (m, 2 H, 2 C*H*H'N), 4.62–4.71 (m, 2 H, 2 CH*H*'N), 5.31 (dd, J = 9.4 Hz, J = 8.2 Hz, 2 H, 2 C*H*Ar), 5.41 (dd, J = 9.4 Hz, J = 8.2 Hz, 2 H, 2 C*H*Het), 6.95 (d, J = 8.3 Hz, 2 H, 2 5′-H), 7.08–7.12 (m, 6 H, 2 2′-H, 2 3″-H, 2 5″-H), 7.22 (br d, J = 8.3 Hz, 2 H, 2 6′-H), 7.47 (d, J = 7.9 Hz, 4 H, 2 2″-H, 2 6″-H), 7.74 (m, 2 H, 2 6-H), 7.85 (m, 2 H, 2 5-H), 8.27 (d, J = 9.2 Hz, 2 H, 2 4-H), 8.46 (d, J = 8.6 Hz, 2 H, 2 7-H) ppm.

X-ray structural analysis

X-ray diffraction data for crystals **3a**, **3b**, **3c**, **4**, **5**, **5a**, **6**, and **6a** were collected on a SMART-6 K (**4**, **5**, **5a**, **6**, **6a**) or Bruker-D8 Venture (**3a**, **3b**, **3c**) diffractometer using graphite-monochromated Mo-K$_\alpha$ radiation (λ = 0.71073 A) and ω-scan. Absorption correction based on measurement of equivalent reflections was applied.[46]

The structures of the initial compounds **3a**, **3b**, **3c**, **4**, **5**, and **5a** were solved by direct methods and refined by full matrix least-squares on F^2 with anisotropic thermal parameters for all non-hydrogen atoms (except O atoms of disordered hydroquinone in **3b** and SO_3 group in **5**). In all these structures H atoms were placed in calculated positions and refined using a riding model in **3a**, **3b**, **3c**, **4**, and **5**. In **5a** H atoms were refined in isotropic approximation.

Structures of PCA products **6** and **6a** also were solved by direct methods. Structure **6a** simultaneously contains initial compound **5** and cyclobutane *rctt*-**6** in the molar ratio 6 : 1.

Structures **6** and **6a** were refined in anisotropic approximation for all non-hydrogen atoms. Atoms H were placed in calculated positions and refined using a riding model.

All the calculations were performed using SHELXTL-Plus[47] and Olex-2 (ref. 48) software. A summary of the crystallographic data and structure determination parameters is provided in Tables 1 and 2.

The experimental data for all structures are deposited in the Cambridge Crystallographic Data Centre (CCDC) registration numbers are 1474550 (**3a**), 1474551 (**3b**), 1474552 (**3c**), 1474553 (**4**), 1474554 (**5**), 1474558 (**5a**), 1474555 (**6**), and 1474556 (**6a**).

Acknowledgements

This work was supported by the Russian Foundation for Basic Research (no. 14-03-00012) and Photochemistry Center of the Russian Academy of Sciences. L. G. K. thanks the Royal Society of Chemistry for International Authors Grant.

Notes and references

1 G. M. J. Schmidt, *Pure Appl. Chem.*, 1971, **27**, 647.
2 V. Ramamurthy and K. Venkatesan, *Chem. Rev.*, 1987, **87**, 433.
3 *Photochemistry in Organized and Constrained Media*, ed. V. Ramamurthy, VCH, New York, 1991.
4 M. V. Alfimov, S. P. Gromov, O. B. Stanislavskii, E. N. Ushakov and O. A. Fedorova, *Russ. Chem. Bull.*, 1993, **42**, 1385.
5 E. N. Ushakov, S. P. Gromov, A. V. Buevich, I. I. Baskin, O. A. Fedorova, A. I. Vedernikov, M. V. Alfimov, B. Eliasson and U. Edlund, *J. Chem. Soc., Perkin Trans. 2*, 1999, 601.
6 C.-H. Huang and D. M. Bassani, *Eur. J. Org. Chem.*, 2005, 4041.

7 M. Nagarathinam and J. J. Vittal, *Macromol. Rapid Commun.*, 2006, **27**, 1091.
8 J. Svoboda and B. König, *Chem. Rev.*, 2006, **106**, 5413.
9 S. P. Gromov, *Russ. Chem. Bull.*, 2008, **57**, 1325.
10 N. Hoffmann, *Chem. Rev.*, 2008, **108**, 1052.
11 L. R. MacGillivray, G. S. Papaefstathiou, T. Friščić, T. D. Hamilton, D.-K. Bučar, Q. Chu, D. B. Varshney and I. G. Georgiev, *Acc. Chem. Res.*, 2008, **41**, 280.
12 S. P. Gromov, A. I. Vedernikov, L. G. Kuz'mina, D. V. Kondratuk, S. K. Sazonov, Yu. A. Strelenko, M. V. Alfimov and J. A. K. Howard, *Eur. J. Org. Chem.*, 2010, 2587.
13 Y. Sonoda, *Molecules*, 2011, **16**, 119.
14 T. Bach and J. P. Hehn, *Angew. Chem., Int. Ed.*, 2011, **50**, 1000.
15 K. Biradha and R. Santra, *Chem. Soc. Rev.*, 2013, **42**, 950.
16 N. Vallavoju and J. Sivaguru, *Chem. Soc. Rev.*, 2014, **43**, 4084.
17 B. Bibal, C. Mongin and D. M. Bassani, *Chem. Soc. Rev.*, 2014, **43**, 4179.
18 R. Medishetty, A. Husain, Z. Bai, T. Runčevski, R. E. Dinnebier, P. Naumov and J. J. Vittal, *Angew. Chem., Int. Ed.*, 2014, **53**, 5907.
19 T. Runčevski, M. Blanco-Lomas, M. Marazzi, M. Cejuela, D. Sampedro and R. E. Dinnebier, *Angew. Chem., Int. Ed.*, 2014, **53**, 6738.
20 A. Chanthapally, H. Yang, H. S. Quah, R. D. Webster, M. K. Schreyer, M. W. Wong and J. J. Vittal, *Chem. – Eur. J.*, 2014, **20**, 15702.
21 L. G. Kuz'mina, A. I. Vedernikov, A. V. Churakov, E. Kh. Lermontova, J. A. K. Howard, M. V. Alfimov and S. P. Gromov, *CrystEngComm*, 2014, **16**, 5364.
22 D. A. Ivanov, N. Kh. Petrov, M. V. Alfimov, A. I. Vedernikov and S. P. Gromov, *High Energy Chem.*, 2014, **48**, 253.
23 S.-Y. Yang, X.-L. Deng, R.-F. Jin, P. Naumov, M. K. Panda, R.-B. Huang, L.-S. Zheng and B. K. Teo, *J. Am. Chem. Soc.*, 2014, **136**, 558.
24 A. A. Parent, D. H. Ess and J. A. Katzenellenbogen, *J. Org. Chem.*, 2014, **79**, 5448.
25 S. P. Gromov, A. I. Vedernikov, N. A. Lobova, L. G. Kuz'mina, S. N. Dmitrieva, Yu. A. Strelenko and J. A. K. Howard, *J. Org. Chem.*, 2014, **79**, 11416.
26 K. M. Hutchins, J. C. Sumrak and L. R. MacGillivray, *Org. Lett.*, 2014, **16**, 1052.
27 S. C. Coote, A. Pöthig and T. Bach, *Chem. – Eur. J.*, 2015, **21**, 6906.
28 Q. Liu, F.-P. Zhu, X.-L. Jin, X.-J. Wang, H. Chen and L.-Z. Wu, *Chem. – Eur. J.*, 2015, **21**, 10326.
29 A. R. Clements and M. Pattabiraman, *J. Photochem. Photobiol., A*, 2015, **297**, 1.
30 V. Ramamurthy and B. Mondal, *J. Photochem. Photobiol., C*, 2015, **23**, 68.
31 M. F. Budyka, T. N. Gavrishova, N. I. Potashova and A. V. Chernyak, *Mendeleev Commun.*, 2015, **25**, 106.
32 E. N. Ushakov and S. P. Gromov, *Russ. Chem. Rev.*, 2015, **84**, 787.
33 F. Li, J. Zhuang, G. Jiang, H. Tang, A. Xia, L. Jiang, Y. Song, Y. Li and D. Zhu, *Chem. Mater.*, 2008, **20**, 1194.
34 A. Papagni, P. Del Buttero, C. Bertarelli, L. Miozzo, M. Moret, M. T. Pryce and S. Rizzato, *New J. Chem.*, 2010, **34**, 2612.
35 J.-K. Sun, W. Li, C. Chen, C.-X. Ren, D.-M. Pan and J. Zhang, *Angew. Chem., Int. Ed.*, 2013, **52**, 6653.
36 K. M. Hutchins, T. P. Rupasinghe, L. R. Ditzler, D. C. Swenson, J. R. G. Sander, J. Baltrusaitis, A. V. Tivanski and L. R. MacGillivray, *J. Am. Chem. Soc.*, 2014, **136**, 6778.
37 L. G. Kuz'mina, A. I. Vedernikov, E. Kh. Lermontova, J. A. K. Howard, M. V. Alfimov and S. P. Gromov, *Russ. Chem. Bull.*, 2013, **62**, 1726.
38 L. G. Kuz'mina, A. I. Vedernikov, J. A. K. Howard, M. V. Alfimov and S. P. Gromov, *CrystEngComm*, 2015, **17**, 4584.
39 K. Müller-Dethlefs and P. Hobza, *Chem. Rev.*, 2000, **100**, 143.
40 M. O. Sinnokrot and C. D. Sherrill, *J. Am. Chem. Soc.*, 2004, **126**, 7690.
41 L. G. Kuz'mina, A. I. Vedernikov, N. A. Lobova, A. V. Churakov, J. A. K. Howard, M. V. Alfimov and S. P. Gromov, *New J. Chem.*, 2007, **31**, 980.
42 L. G. Kuz'mina, A. I. Vedernikov, N. A. Lobova, S. K. Sazonov, S. S. Basok, J. A. K. Howard and S. P. Gromov, *Russ. Chem. Bull.*, 2009, **58**, 1192.
43 L. G. Kuz'mina, A. I. Vedernikov, S. K. Sazonov, N. A. Lobova, A. V. Churakov, E. Kh. Lermontova, J. A. K. Howard, M. V. Alfimov and S. P. Gromov, *Russ. Chem. Bull.*, 2011, **60**, 1734.
44 M. Koral, D. Bonis, A. J. Fusco, P. Dougherty, A. Leifer and J. E. LuValle, *J. Chem. Eng. Data*, 1964, **9**, 406.
45 A. I. Vedernikov, L. G. Kuz'mina, S. K. Sazonov, N. A. Lobova, P. S. Loginov, A. V. Churakov, Yu. A. Strelenko, J. A. K. Howard, M. V. Alfimov and S. P. Gromov, *Russ. Chem. Bull.*, 2007, **56**, 1860.
46 G. M. Sheldrick, *SADABS, Program for Scaling and Correction of Area Detector Data*, University of Göttingen, Germany, 1997.
47 *SHELXTL-Plus, Version 5.10*, Bruker AXS Inc., Madison, Wisconsin (USA), 1997.
48 O. V. Dolomanov, L. J. Bourhis, R. J. Gildea, J. A. K. Howard and H. Puschmann, *J. Appl. Crystallogr.*, 2009, **42**, 339.